Activin A rescues preterm brain injury through a novel Noggin/BMP4/Id2 signaling pathway

XIAOJUAN SU, JUNJIE YING, DONGQIONG XIAO, XIA QIU, SHIPING LI, FENGYAN ZHAO and JUN TANG

Department of Pediatrics/Key Laboratory of Birth Defects and Related Diseases of Women and Children (Ministry of Education), West China Second University Hospital, Sichuan University, Chengdu, Sichuan 610041, P.R. China

Received October 14, 2022; Accepted December 7, 2022

DOI: 10.3892/ijmm.2022.5215

Abstract. Activin A (Act A) has been reported to promote oligodendrocyte progenitor cell (OPC) differentiation *in vitro* and improve neurological outcomes in adult mice. However, the roles and mechanisms of action of Act A in preterm brain injury are unknown. In the present study, P5 rats were subjected to hypoxia-ischemia to establish a neonatal white matter injury (WMI) model and Act A was injected via the lateral ventricle. Pathological characteristics, OPC differentiation, myelination, and neurological performance were analyzed. Further, the involvement of the Noggin/BMP4/Id2 signaling pathway in the roles of Act A in WMI was explored. Act A attenuated pathological damage, promoted OPC differentiation, enhanced myelin sheath and myelinated axon formation, and improved neurological performance of WMI rats. Moreover, Act A enhanced noggin expression, which, in turn, inhibited the expression of bone morphogenetic protein 4 (BMP4) and inhibitor of DNA binding 2 (Id2). Furthermore, upregulation of Id2 completely abolished the rescue effects of Act A in WMI rats. In conclusion, the present findings suggested that Act A rescues preterm brain injury via targeting a novel Noggin/BMP4/Id2 signaling pathway.

Introduction

White matter injury (WMI) is a major form of preterm brain injury induced by hypoxic ischemia (HI), particularly between 23 and 32 weeks of gestational age, a period that corresponds to the peak of myelination (1). WMI impairs the differentiation ability of oligodendrocyte progenitor cells (OPCs), resulting in oligodendrocyte (OL) deficiency and deficits in myelination, leading to cognitive and behavioral disorders that negatively impact survival and quality of life in children (2,3). In this regard, impaired differentiation ability of OPCs constitutes a key mechanism of WMI pathogenesis. Currently, clinical treatments for mature OL deficiency are limited. Hence, there is an urgent need to explore strategies to promote the differentiation and maturation of OPCs, which may provide novel therapeutic approaches for WMI.

The myelin sheath is a major component of white matter and is formed by mature OLs that differentiate from OPCs (4). The myelinating microenvironment is a key factor that hinders differentiation and maturation of OPCs after WMI (5). Therefore, optimizing the myelinating microenvironment, which is formed by a network of neuronal astrocytes and microglial blood vessels, is an important means to promote the differentiation and maturation of OPCs (5). Based on extant literature and previous *in vitro* experiments by the authors, several endogenous molecules have been identified to directly or indirectly improve the myelinating microenvironment and promote the differentiation of human OPCs (5). Among them, Activin A (Act A) plays a key role (6). Act A is a widely expressed homodimer composed of two β_A chains. Sequence analysis has revealed that the β subunit of Act A possesses the typical structural features of the transforming growth factor-β superfamily, and the mature human β_A chain of Act A has 100% amino acid sequence identity in cattle, cats, mice, and pigs, highlighting its highly conserved structure (7). In the nervous system, Act A is secreted by neurons and glial cells, which exert neuroprotective effects. A previous study reported that treatment of OPCs cultured *in vitro* with recombinant Act A protein promoted OPC proliferation and differentiation (6). Further, another study reported that Act A improved neurological outcomes by regulating OPC function in adult male mice (8). Collectively, these reports suggested that Act A may be used in the treatment of myelination disorders. However, the roles and mechanisms of action of Act A in preterm brain injury remain unclear. Given the considerable differences between the adult and preterm brains in responses to external stimuli such as HI, it is essential to examine the effects of Act A in the preterm brain. Therefore, the present study aimed to investigate whether exogenous Act A treatment could enhance OPC differentiation in WMI and to explore the underlying mechanisms.

Correspondence to: Professor Jun Tang, Department of Pediatrics/Key Laboratory of Birth Defects and Related Diseases of Women and Children (Ministry of Education), West China Second University Hospital, Sichuan University, Section 3, 20 South Renmin Road, Chengdu, Sichuan 610041, P.R. China
E-mail: tj1234753@sina.com

Key words: preterm brain injury, hypoxia-ischemia, white matter injury, Activin A, Noggin/BMP4/Id2 signaling pathway, oligodendrocyte progenitor cells

Materials and methods

Animals. Brain development of newborn Sprague-Dawley (SD) rats aged 2-5 days has been reported to be consistent with that of human fetuses aged 23-32 weeks (9,10). In order to avoid the effects of high mortality on the modeling process of young rats, postnatal day 5 (P5) SD rats were used for modeling.

In the present study, a total of 1,335 specific-pathogen-free, P5 healthy male (SD) rats (average weight: 10-15 g) were purchased from Sichuan Dashuo Animal Science and Technology Co., Ltd. (Chengdu, China). A total of six rats were used for each group and each group was maintained with one cage under a 12-h light/dark cycle. The relative humidity was controlled at 40-70% and the temperature at 23±2˚C, with ad libitum access to food and water. During the experimental period (from P5 to P35), if any rat began to show signs of inability to move or eat, ruffled fur or self-mutilation, they were immediately sacrificed. In addition, animals were euthanized to prevent further suffering if they were unable to stand or displayed agonal breathing, severe muscular atrophy, severe ulcers or uncontrolled bleeding. The rats with unsuccessful modeling were euthanized by cervical dislocation under anesthesia for euthanasia. Complete cardiac and respiratory arrest were observed to verify animal death. It was confirmed that the animal studies abided to all of the animal welfare, including efforts to minimize suffering and distress, use of analgesics or anesthetics (including the dose and duration), or special housing conditions. All animal experiments were approved (approval no. WCSUH21-2018-034) by the Sichuan University Committee on Animal Research (Chengdu, China) and complied with the ARRIVE guidelines.

WMI modeling. The rats were randomly divided into WMI and Sham groups. The WMI group was established using the following procedure as previously described (11). First, P5 neonatal rats were fixed on their backs after general anesthesia. A 1-cm longitudinal incision was made in the neck, and the right carotid artery was exposed and ligated after separation from glands and muscle tissue. After surgery, the rats were placed in an incubator for 30 min to recover. Subsequently, the rats were placed in an 8%-oxygen and 92%-nitrogen cabin (8% O_2 and 92% N_2) with a gas flow rate of 3 l/min for 2 h to induce WMI. Rats were maintained on a heating pad during surgical procedures to maintain body temperature at 36-37˚C. Rats in the Sham group were only subjected to neck incision to dissociate the right carotid artery, without ligation or hypoxia. Following surgery, all neonatal rat pups were returned to their cages.

Establishment of testing and control groups. After 24 h of WMI modeling, the WMI group was treated with Act A or PBS to establish the Act A and PBS groups as testing and control groups, respectively. To establish the Act A and PBS groups, rats were injected with 5 μl of Act A (12.5, 25, and 50 mg/kg) or PBS, respectively, using a Hamilton syringe needle via the lateral ventricle (LV), located 2 mm posterior and 2 mm lateral (right) from bregma to a needle depth of 2 mm. Next, the Act A group was treated with Id2-overexpressing lentiviral vector and mock-vehicle to establish the Id2 and V groups as the testing and control groups, respectively. To establish the Id2 and V groups, rats in the Act A group were injected with 4 μl of Id2 ($1x10^9$ TU/ml)-overexpressing lentiviral vector or mock-vehicle into the lateral ventricle using a Hamilton syringe needle 6 h after Act A treatment.

Hematoxylin & eosin staining. On P7, the rats were sequentially perfused with 0.9% normal saline and 4% paraformaldehyde (100 ml each), after which tissues were extracted and post-fixed in a 4% paraformaldehyde solution for 24-36 h at 4˚C. Then, the tissues were paraffin-embedded and 5-mm thick serial sections were made in the coronal plane. A total three 3 sections containing the corpus callosum (CC) (0.26-1.80 mm behind the anterior fontanelle according to the rat brain atlas) were selected for analysis. Finally, the sectioned tissues were stained with hematoxylin & eosin (H&E) and were observed using an inverted optical microscope (Leica Microsystems GmbH). Randomly selected fields (n=4) were examined in each animal. A total of six animals per group were analyzed.

Immunofluorescence staining. The rat brains were obtained at set time points (P7, P14, P21, P28, and P35) and post-fixed in 4% paraformaldehyde at 4˚C for at least 48 h, then embedded in 2-3% agarose. Coronal brain sections were cut using an oscillating tissue slicer (Leica Microsystems GmbH). A total of three sections containing the CC were selected for analysis. The sections were first washed in PBS and incubated in 0.3% Triton X-100 at room temperature for 30 min and then incubated for 1 h in fetal calf serum (Gibco; Thermo Fisher Scientific, Inc.) to inhibit non-specific binding. Next, the brain sections were incubated with primary antibodies (Table I) at 4˚C overnight, then incubated for 2 h at room temperature with secondary antibodies (Table I). Finally, fluorescence imaging was performed using a confocal laser scanning microscope (Olympus Corporation) and FV-ASW-3.1 software (Olympus Corporation), and mean fluorescence intensity or positive cells were quantified. Mean fluorescence intensity was defined as the ratio between the sum of the integral optical density of the target protein and area. Positive cells and mean fluorescence intensity were quantified for each field with a x40 objective lens (field size, 0.24 mm^2) using ImageJ 1.8.0.345 software (National Institutes of Health). Randomly selected fields (n=6) from the CC were examined in each animal. A total of six animals per group were analyzed.

Western blot analysis. Isolated CC tissues were treated with a brain tissue protein extraction kit (cat. no. BB-31227-1; Chengdu beibo; http://beibokit.com/). Lysates were centrifuged at 12,000 x g for 30 min at 4˚C. Protein concentration was determined using a BCA protein assay kit (Pierce; Thermo Fisher Scientific, Inc.). Protein samples (50 μg per lane) were separated on sodium dodecyl sulfate-polyacrylamide gels (12%). Next, the proteins were transferred to polyvinylidene fluoride or polyvinylidene difluoride membranes, blocked [2.5 g skim milk powder dissolved in 50 ml TBST (0.1% Tween 20)] at room temperature for 1 h, and incubated overnight at 4˚C with primary antibodies (Table I). The next day, the membranes were washed and then incubated with secondary antibodies (Table I) in blocking solution for 1 h. Finally, the membranes were exposed to obtain signals of the bound antibody signals. Quantification was performed using ImageJ

Table I. Information of the antibodies used in immunofluorescence and western blot experiments.

		Antibody name	Host species	Dilution	Cat. no./Supplier
Immunofluorescence	Primary antibody	Id2	Rabbit	1:500	NBP2-27194/Novus Biologicals, LLC
		BMP4	Rabbit	1:500	ab39973/Abcam
		Olig2	Rabbit	1:500	AB9610/Abcam
		Ki67	Rabbit	1:500	ab15580/Abcam
		Vimentin	Mouse	1:200	ab8978/Abcam
		CC3	Rabbit	1:500	PA5-77887/Invitrogen; Thermo Fisher Scientific, Inc.
		NG2	Rabbit	1:200	AB5320/Abcam
		O4	Mouse	1:25	MAB345/MilliporeSigma
		CC-1	Mouse	1:200	ab16794/Abcam
		MBP	Mouse	1:1,000	ARG10722/Arigo Biolaboratories, Inc.
		MAG	Rabbit	1:100	ab89780/Abcam
		PLP	Rabbit	1:1,000	ab28486/Abcam
		Tau1	Mouse	1:1,000	MAB3420/MilliporeSigma
		SMI31	Mouse	1:1,000	SMI31P/BioLegend, Inc.
		SMI312	Mouse	1:1,000	837904/BioLegend, Inc.
	Secondary antibody	Cy3/488-conjugated	Donkey anti-rabbit/ mouse IgG	1:500	712-166-150/715-165-150 711-545-152/715-545-150/ Jackson ImmunoResearch Laboratories, Inc.
Western blot analysis	Primary antibody	Act A	Rabbit	1:500	NBP1-30928/Novus Biologicals, LLC
		MBP	Mouse	1:500	ARG10722/Arigobio Biolaboratories, Inc.
		MAG	Rabbit	1:100	ab89780/Abcam
		PLP	Rabbit	1:500	ab28486/Abcam
		Tau1	Mouse	1:500	MAB3420/MilliporeSigma
		SMI31	Mouse	1:500	SMI31P/BioLegend, Inc.
		SMI312	Mouse	1:500	837904/BioLegend, Inc.
		Noggin	Mouse	1:200	ab239520/Abcam
		BMP4	Rabbit	1:500	ab39973/Abcam
		Id2	Rabbit	1:500	NBP2-27194/Novus Biologicals, LLC
		Actin	Mouse	1:5,000	sc-2357/Santa Cruz Biotechnology, Inc.
	Secondary antibody	HRP-conjugated	Goat anti-rabbit/ mouse IgG	1:5,000	sc-2004/sc-2005/Santa Cruz Biotechnology, Inc.

Id2, inhibitor of DNA binding 2; MBP, myelin basic protein; PLP, proteolipid protein; MAG, myelin-associated glycoprotein; Act A, Activin A.

software (National Institutes of Health). The relative expression levels of target proteins were calculated as the target protein integrated density values (IDVs) relative to actin IDVs.

Electron microscopy (EM). On P35, rat brains were obtained and sectioned into ~1 mm^3 blocks containing the CC area. The sectioned tissue was pre-fixed with a mixed solution of 3% glutaraldehyde at 4˚C for 48 h, post-fixed in 1% osmium tetroxide, dehydrated in an acetone series 2 h at room temperature, filtrated in Epox 812, and embedded with EMBed 812 (cat. no. 90529-77-4; SPI; https://www.2spi.com/category/chemicals/). Next, semi-thin sections were stained with methylene blue for 8 min at room temperature, and ultrathin sections were stained with uranyl acetate and lead citrate for 8 min at

room temperature. Finally, the ultrathin sections were examined using a transmission electron microscope (H-600IV; Hitachi, Ltd.). Myelinated axons in each field were quantified using Image-Pro Plus 6.0 software (Media Cybernetics, Inc.). A total of four randomly selected fields from the CC were examined in each animal. A total of six animals per group were analyzed.

Morris water maze (MWM) test. Neurological performance was verified using the MWM test from P29 to P35. The testing apparatus comprised a circular tank (1.5 m in diameter), location-constant platform (14 cm in diameter) placed 1.5 cm under the surface of the water, and an overhead camera. The water temperature was maintained at 25±1˚C during testing. The test consists of two parts, namely place navigation training and space exploration, both of which are aimed to test spatial learning and memory ability. Place navigation training was conducted during the first 6 days (P29-P34), for which the rats were trained to swim in the four alternating quadrants. The rats were allowed to swim in the water from each quadrant for 120 sec. If the platform was successfully found during this period, the escape latency was recorded as the time taken for rats to find the platform. Rats that failed to find the platform within 120 sec were guided to it by a researcher and allowed to stay on the platform for 30 sec, and the escape latency was recorded as 120 sec. The time in which the rats found the platform in each training session was recorded. The average latency period for the four quadrants was computed as a daily final score representing the ability to acquire spatial information. The platform was removed, and a space navigation test was conducted on P35 to assess memory retention ability 24 h after the final place navigation training. The rats were allowed to swim freely in the tank for 120 sec from the third quadrant starting point. The trials were recorded using a video camera on the ceiling, and the platform crossing time was calculated and analyzed using a tracking system (Mengtai, China).

Quantification and statistical analysis. All images were acquired from the same CC area. All data are presented as mean ± standard deviation (SD). All graphs were generated using GraphPad Prism 8.0 (GraphPad Software, Inc.). Comparison between two groups was performed using an unpaired Student's t-test. Analysis of variance (ANOVA) was used to compare more than two groups, followed by the Student's t-test if homogeneity of variance was assumed or by Dunnett's test if homogeneity of variance was not assumed. A total of six animals were used for each group, each experiment was conducted for three times, and totally ~1,335 rats were used in the present study. All statistical analyses were performed using SPSS 23.0 (IBM Corp.). $P<0.05$ was considered to indicate a statistically significant difference.

Results

HI attenuates Act A expression in neonatal rat brains. Based on brain developmental characteristics in rats, a time course for each assay was set, which is presented as a schematic diagram in Fig. 1A. Western blot experiments were first conducted to detect the endogenous expression of Act A after HI at P21 by using the isolated CC tissues. Western blotting revealed that Act A expression was lower in the WMI group than in the Sham group (Fig. 1B), indicating that HI reduced Act A expression in neonatal rats.

Act A treatment alleviates pathological damage after WMI. To detect the distribution of Act A after injection via the LV, Act A-enhanced green fluorescent protein (EGFP) protein was constructed and immunofluorescence tracing was performed. Fluorescence scanning revealed that Act A-EGFP was distributed in the cortex and white matter (including CC) from days 1 to 28 after LV injection (Fig. 1C). To select the optimal usage of Act A for WMI therapy, three dose concentrations were used (low, 12.5 mg/kg; medium, 25 mg/kg; and high, 50 mg/kg) and three time points (12, 24 and 48 h) for Act A administration after HI. Pathological changes in the brain white matter and liver were examined via H&E staining and body weights on P14 were analyzed. H&E staining revealed that Act A treatment decreased the loosely arranged nerve fibers and cell edema in the CC area, which exhibited with markedly less tissue vacuolization and nuclear fragmentation and liquefaction 24 h after HI, suggesting that Act A treatment ameliorated the pathological characteristics of WMI (Fig. 1D). Further analysis indicated that the medium and high doses of Act A treatment showed more effective pathological improvement when compared with that treated with the low dose, though there was no significant difference in pathological improvement effects between the medium and high doses (Fig. 1D). However, hepatic H&E staining on P21 and body weight analysis revealed that the high dose of Act A treatment led to less hepatic lobule and had lower body weight and poor state in rats (Fig. 1D). Therefore, subsequent experiments were performed with a medium dose of Act A (25 mg/kg). To detect the overall expression levels of Act A in the brain after exogenous Act A injection, western blotting was conducted on P6. Act A was abundantly expressed in the Act A group than in the PBS group (Fig. 1E). Collectively, these results suggested that exogenous Act A supplementation alleviated pathological damage in WMI.

Act A treatment promotes OPC differentiation after WMI. Next, it was examined whether Act A contributes to the differentiation of OPCs to OLs. On P7 and P14, the number of OPCs in white matter was quantified via double immunostaining with mature-oligodendrocyte marker oligodendrocyte transcription factor (Olig2) and OPC-specific marker neural/glial antigen 2 (NG2) in the experimental groups. The number of NG2/Olig2-positive cells and mean NG2/Olig2 fluorescence intensity at both time points were significantly higher in the Act A group than in the PBS group (Fig. 2A). On P14 and P21, the number of pre-OLs was quantified in the CC by double immunostaining with Olig2 and the pre-OL-specific marker O4 in the experimental groups. The number of O4/Olig2-positive cells and mean O4/Olig2 fluorescence intensity at both time points were significantly higher in the Act A group than in the PBS group (Fig. 2B). Further, on P21 and P28, double immunofluorescence staining was performed with the mature OL marker CC1 with Olig2 in the CC. The number of CC1/Olig2-positive cells and mean CC1/Olig2 fluorescence intensity were significantly higher in the Act A group

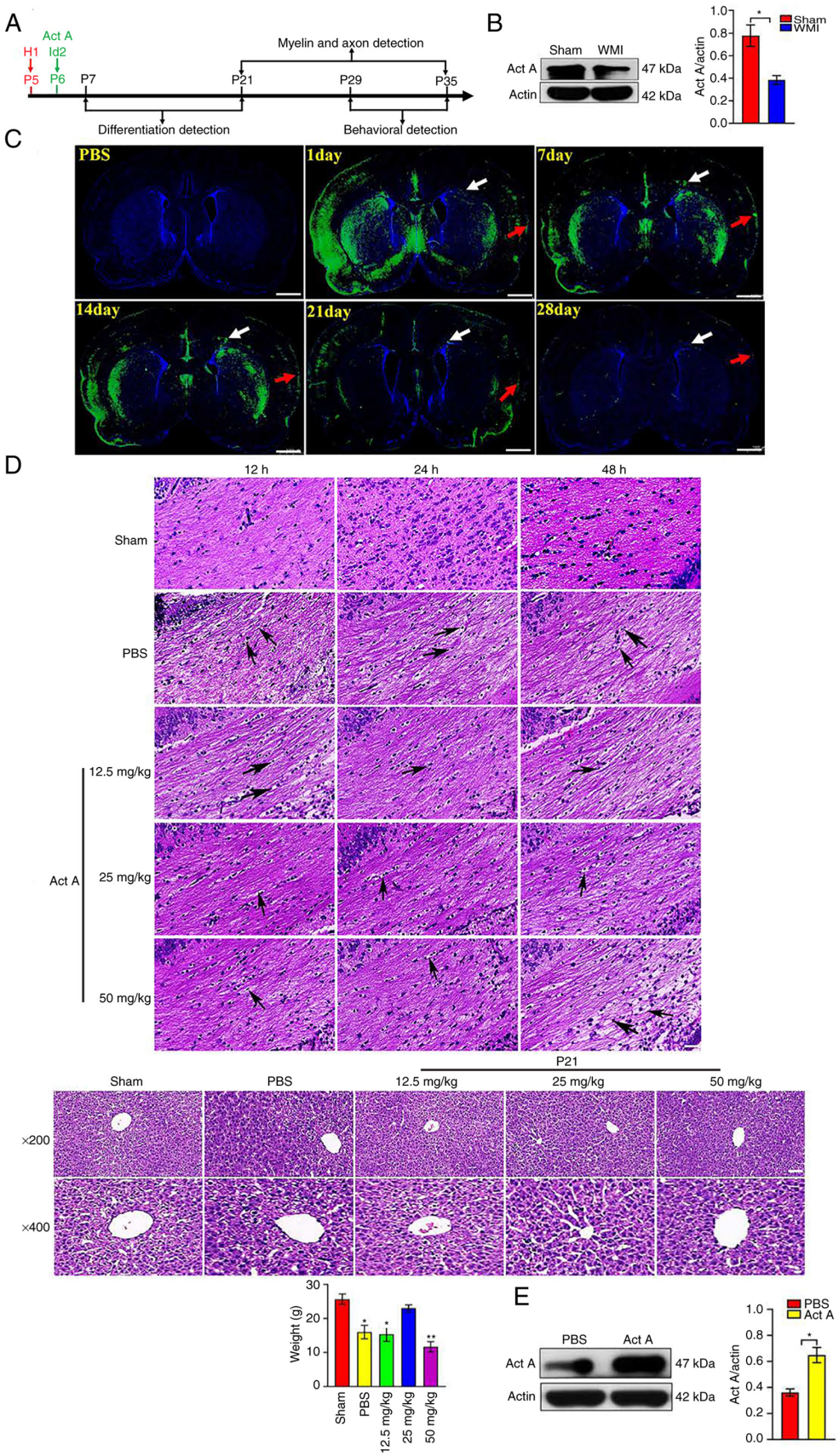

Figure 1. Act A treatment attenuates the pathological damages in WMI. (A) Schematic diagram displaying the design of the animal experiment. (B) Detection of Act A expression via western blot in the Sham and WMI groups at P21 by using the isolated CC tissues. (C) Immunofluorescence detection for Act A-EGFP after injected via the lateral ventricle. Arrows indicate the Act A-EGFP (green fluorescence) positive area. Scale bar, 1,000 μm. (D) H&E staining to evaluate the histopathologic characteristics of the CC area and the liver in Sham, PBS and Act A groups. Scale bar, 20 μm. Arrows indicate the vacuolization and nuclear fragmentation. Weight statistics of P14 in each group. PBS/Act A, group with PBS/Act A injected after WMI. (E) Detection of Act A expression after Act A treatment by western blot analysis at P21 by using the isolated CC tissues. *P<0.05 and **P<0.001. WMI, white matter injury; Act A, Activin A; P, postnatal day; CC, corpus callosum.

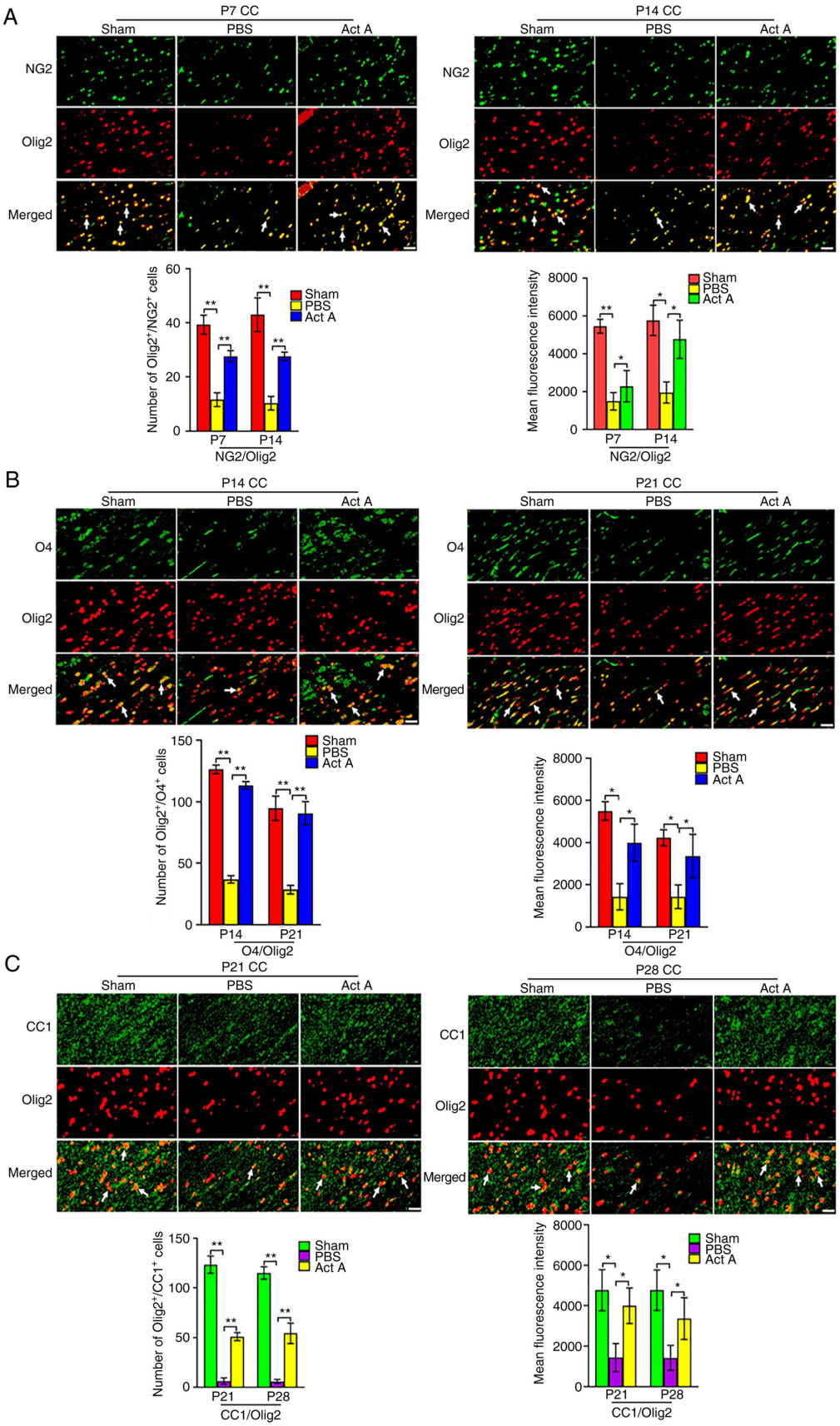

Figure 2. Act A treatment promotes OPC differentiation in WMI. (A) Representative immunofluorescence images and quantification of NG2 (green) expression via double staining with Olig2 (red) at P7 and P14. Arrows indicate the NG2/Olig2 (yellow) positive cells. NG2, a OPCs marker. Scale bar, 20 μm. (B) Representative immunofluorescence images and quantification of O4 (green) expression via double staining with Olig2 (red) at P14 and P21. Arrows indicate the O4/Olig2 (yellow) positive cells. O4, a marker of pre-oligodendrocytes. Scale bar, 20 μm. (C) Representative immunofluorescence images and quantification of CC1 (green) expression via double staining with Olig2 (red) at P21 and P28. Arrows indicate the CC1/Olig2 (yellow) positive cells. CC1, Anti-APC (Activated protein C), a marker of mature oligodendrocytes. Scale bar, 20 μm. *P<0.05 and **P<0.001. OPC, oligodendrocyte progenitor cell; WMI, white matter injury; Olig2, oligodendrocyte transcription factor; Act A, Activin A; NG2, neural/glial antigen 2; CC, corpus callosum.

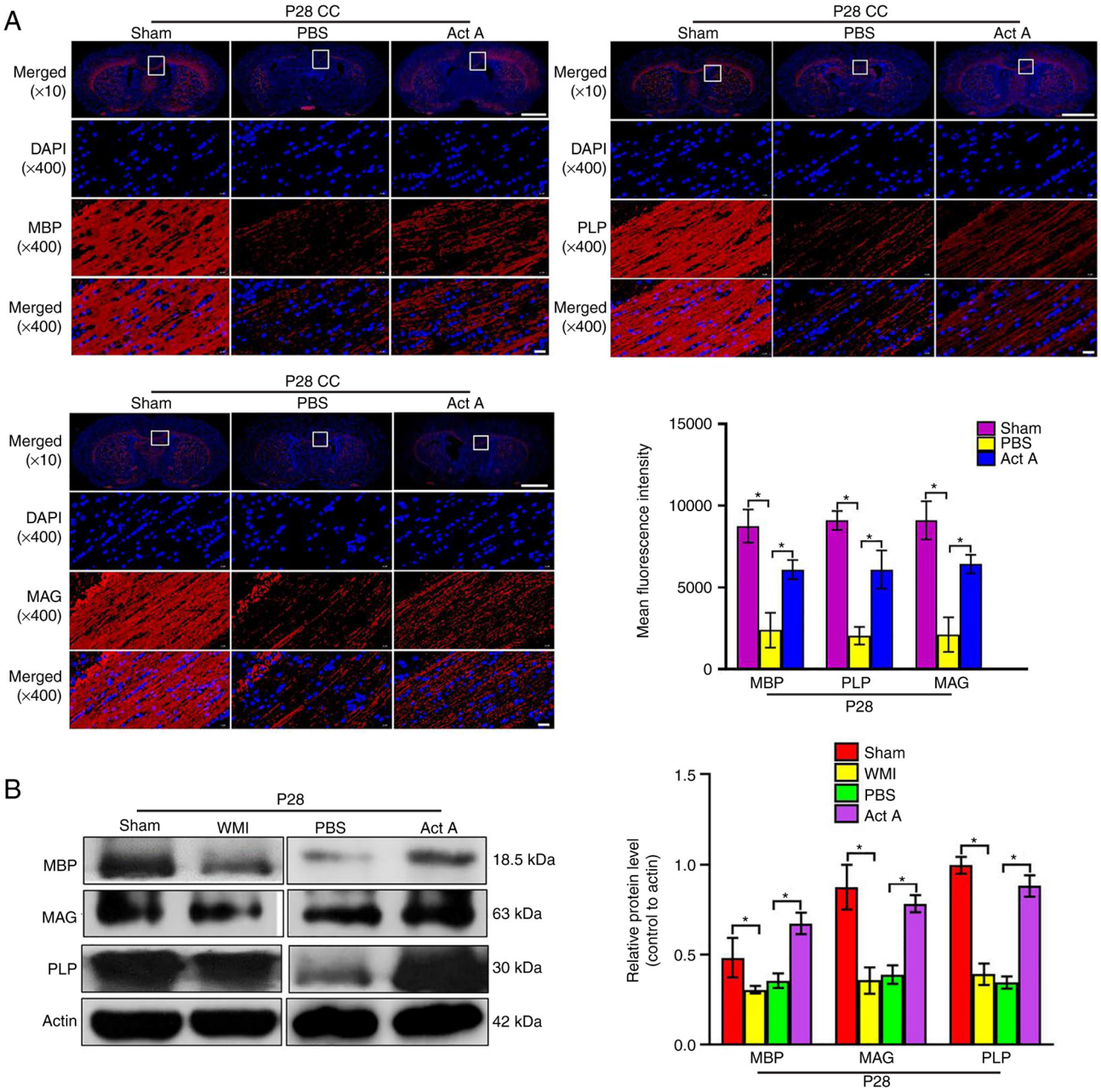

Figure 3. Act A treatment promotes the myelination in WMI. (A) Representative immunofluorescence images and quantification of the expression of the myelin sheath markers MBP, PLP and MAG (red) at P28. Cell nuclei were labeled with DAPI (blue). The mean fluorescence intensity of MBP, PLP, and MAG was quantified. Scale bar, 1,000 or 20 μm. (B) Western blot analysis and corresponding quantification were conducted to measure the expression of MBP, PLP and MAG at P28. It showed that the expression of MBP, PLP and MAG was significantly enhanced in the Act A group compared with the PBS group. *P<0.05. Act A, Activin A; WMI, white matter injury; MBP, myelin basic protein; PLP, proteolipid protein; MAG, myelin-associated glycoprotein.

than in the PBS group (Fig. 2C). Collectively, these results indicated that Act A promoted OPC differentiation.

Act A treatment promotes myelination and axon formation after WMI. CC myelination was then examined by assessing the expression of myelin basic protein (MBP), proteolipid protein (PLP), and myelin-associated glycoprotein (MAG) using immunofluorescence and western blot analysis. On P28, the expression of MBP, PLP, and MAG was significantly higher in the Act A group than in the PBS group (Fig. 3A and B). Consistent with this, on P35, expression of the axon markers Tau1, SMI31, and SMI312 was significantly higher in the Act A group than in the PBS group (Fig. 4A and B). On P35, EM revealed more myelinated axons in the CC of brains in the Act A group than in the CC of brains in the PBS group (Fig. 4C). Collectively, these results indicated that exogenous Act A supplementation after WMI contributed to myelination and axon formation.

Act A treatment improves neurological performance after WMI. The MWM test was conducted to compare learning and memory abilities among the experimental groups from P29 to P35 by calculating average escape latency and platform crossing times. The average escape latency from P31 was significantly lower in the Act A group than in the PBS group (Fig. 5A). The frequency of platform crossings at P35 was

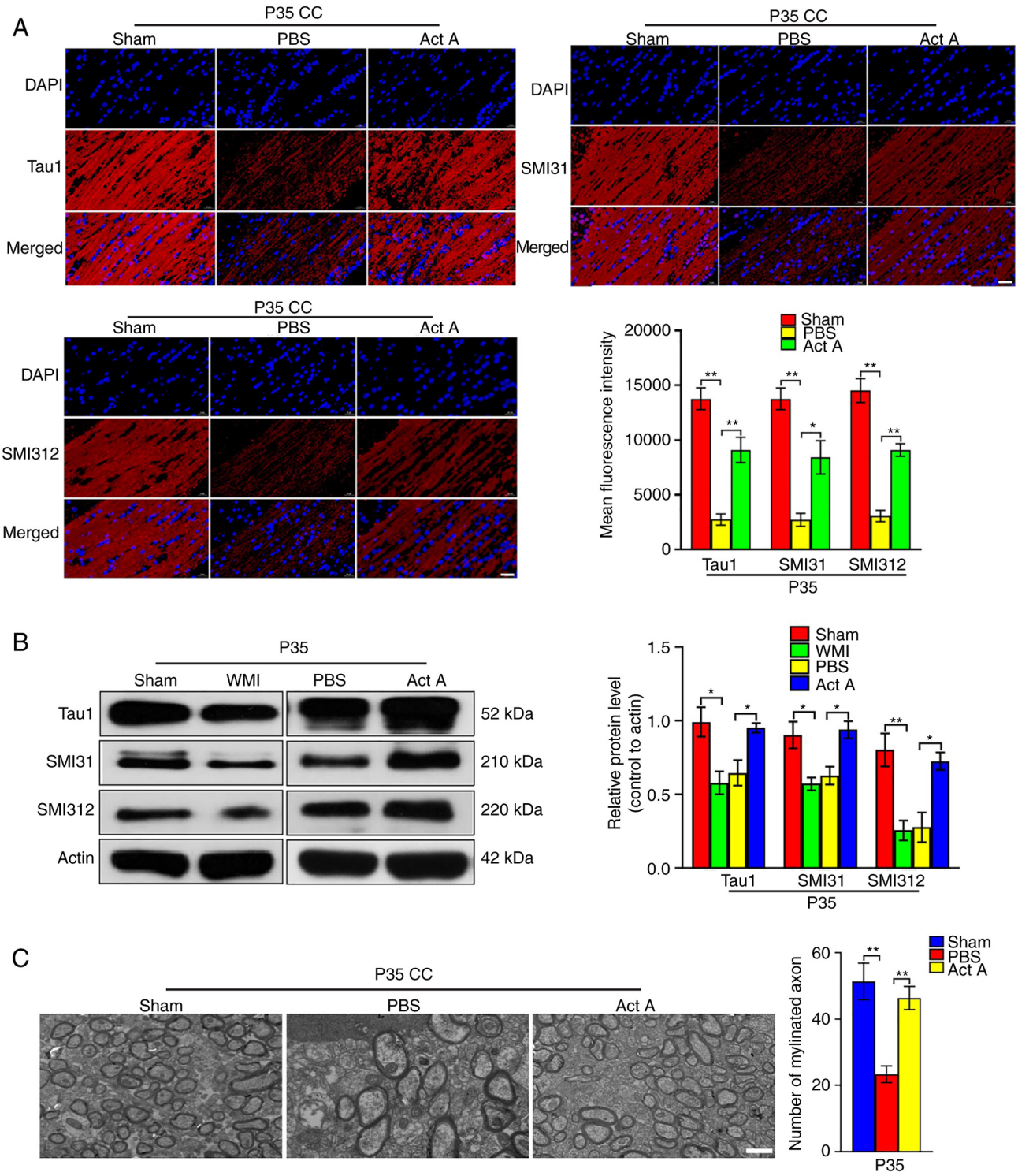

Figure 4. Act A treatment enhances the axon formation in white matter injury. (A) Representative immunofluorescence images and quantification of axons markers Tau1, SMI31, and SMI312 (red) at P35. The mean fluorescence intensity of Tau1, SMI31 and SMI312 was quantified. Scale bar, 20 μm. (B) Western blot analysis and corresponding quantification were performed to measure the expression of Tau1, SMI31, and SMI312 at P35. It showed that the expression of Tau1, SMI31 and SMI312 was significantly increased in the Act A group compared with the PBS group. (C) Representative EM images in the CC at P35. The number of myelinated axons was counted per field using the Image-Pro Plus 6.0 software. It showed that the Act A group with more myelinated axons compared with the PBS group. Scale bar, 2 μm. *P<0.05 and **P<0.001. Act A, Activin A; WMI, white matter injury; CC, corpus callosum.

significantly higher in the Act A group than in the PBS group, whereas no significant difference was observed between the Act A and Sham groups (Fig. 5B). These results suggested that exogenous Act A treatment contributed to improvements in learning and memory.

Act A treatment increases noggin expression and inhibits BMP4/Id2 expression after WMI. Immunofluorescence was performed to detect the expression of bone morphogenetic protein 4 (BMP4) and inhibitor of DNA binding 2 (Id2) in Sham, PBS and Act A groups. Expression of these proteins

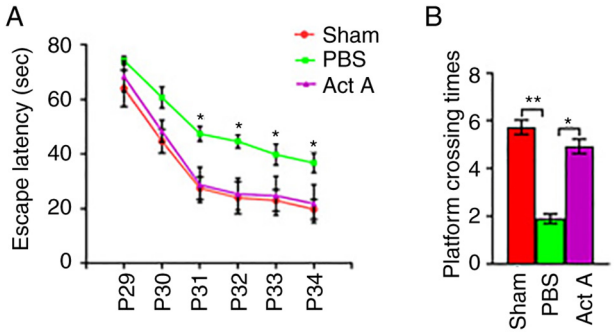

Figure 5. Act A treatment improves the behavioral performance of white matter injury rats. (A) Daily average escape latency of SD rats from P29 to P34. The place navigation test was conducted and the escape latency was calculated to assess the acquisition of spatial information of rats. It showed that the average escape latency was greatly decreased in the Act A group compared with the PBS group. (B) The average platform crossing times of SD rats at P35. The space navigation test was conducted and the platform crossing times were calculated to evaluate the memory retention ability of rats. The frequency of platform crossing was significantly increased in the Act A group compared with the PBS group. *P<0.05 and **P<0.001. Act A, Activin A.

was significantly higher in the PBS group than in the Sham group (Fig. 6A and B) but was significantly decreased after Act A treatment (Fig. 6A and B). Western blot analysis revealed that noggin expression was significantly higher in the Act A group than in the PBS group, whereas both BMP4/Id2 proteins were significantly lower in the Act A group than in the PBS group (Fig. 6C). Next, Id2 was upregulated in the Act A group using an Id2-overexpressing lentiviral vector ($1x10^9$ TU/ml). Fluorescence imaging revealed that Id2-EGFP was distributed in the cortex and white matter (including CC) for up to 4 weeks. On the first day post-injection, Id2-EGFP was observed in the CC (white arrow) and cortex (red arrow). From the 7th to 21st day post-injection, Id2-EGFP fluorescence intensity in the CC and cortex was significantly increased, whereas on the 28th day post-injection, Id2-EGFP fluorescence intensity in the CC and cortex was significantly decreased (Fig. 7A). In addition, immunofluorescence and western blot experiments were performed to detect Id2 expression in the V and Id2 groups. The analysis revealed that Id2 expression was significantly higher in the Id2 group than in the V group (Fig. 7B). H&E staining revealed more white matter vacuolization and nuclear fragmentation in the Id2 group than in the V group (Fig. 7C). Collectively, these results suggested that the beneficial effects of Act A on WMI involved the Noggin/BMP4/Id2 signaling pathway.

Id2 overexpression attenuates the therapeutic effects of Act A on WMI via the Noggin/BMP4/Id2 signaling pathway. The number of immunopositive cells and mean fluorescence intensity for NG2/Olig2 (Fig. 8A), O4/Olig2 (Fig. 8B), and CC1/Olig2 (Fig. 8C) were significantly lower in the Id2 group than in the V group. Furthermore, Id2 upregulation attenuated the expression of MBP, PLP, MAG (Fig. 9A), Tau1, SMI31 and SMI312 (Fig. 9B) after Act A treatment, as indicated by immunofluorescence. Similarly, on P35, EM revealed fewer myelinated axons in the Id2 group than in the V group (Fig. 9C). The MWM test revealed that the average escape latency from P31 was significantly higher in the Id2 group than in the V group (Fig. 10A), and the frequency of platform crossings at P35 was significantly lower in the Id2 group than in the V group (Fig. 10B). Performance was similar between the Id2 and PBS groups, suggesting that Id2 upregulation rescued behavioral dysfunction. Collectively, these results verified that Act A exerted therapeutic effects on WMI via the Noggin/BMP4/Id2 signaling pathway.

Discussion

OPCs constitute the major cell population that is injured in WMI. As such, protecting OPCs constitutes a key strategy for WMI treatment (12). Previous studies have reported the involvement of Act A in the regulation of OPC maturation *in vitro*, which led us to examine its role in WMI *in vivo* (13,14). In an adult rat model of focal cerebral ischemia simulating stroke, expression of Act A around the infarction was higher than that in control rats (15). However, in the current study, it was observed that the expression of endogenous Act A was significantly lower after WMI in newborn rats. This discrepancy may be due to the differences in the age of rats and injury models used. Further, the reduction in Act A expression suggests the involvement of Act A in WMI pathophysiology. Act A is secreted by both neurons and glial cells, which exert neuroprotective effects. In the present study, it was attempted to partially replenish Act A dosage via exogenous administration to compensate for the WMI-induced decrease in Act A levels. Given the presence of the blood-brain barrier (BBB), Act A was injected via the LV in a rat model of WMI. Act A-EGFP tracing experiments revealed that Act A-EGFP protein was distributed in the cerebral cortex and white matter (including the CC) from days 1 to 28 after injection. This indicated that Act A could enter the brain and persist for up to 4 weeks after intra-LV injections, supporting its efficacy after a single administration. To explore the therapeutic time window of Act A, injections were performed before and after modeling, as well as single or continuous multiple injections in a preliminary study. It was observed that the effects of injection before modeling were improved compared with those after modeling. Nevertheless, no differences were observed in the effects of single vs. multiple injections. Given that injections before modeling do not fully recapitulate clinical settings, injections were performed after model establishment. Next, three different concentrations of Act A were analyzed to determine the optimal dosage. H&E staining for the CC showed that three doses of Act A improved the injury when compared with the PBS-treated groups. Further H&E staining for hepatic tissues and body weight analysis demonstrated that the highest dose (50 mg/kg) led to less hepatic lobule and with poor body weight improvement. Furthermore, the body wight in the lowest dosage (12.5 mg/kg) decrease obviously than that in the medium dose (25 mg/kg). Collectively, after careful consideration, it was decided to use the medium dose of Act A to treat the WMI rats. In this regard, exogenous administration of a certain dose of Act A may have rescued vulnerable cell populations, such as OPCs, which, in turn, increased myelin sheath and neural network formation, improved the white matter microenvironment in WMI, and ameliorated WMI-induced diffuse damage. Although LV injections are

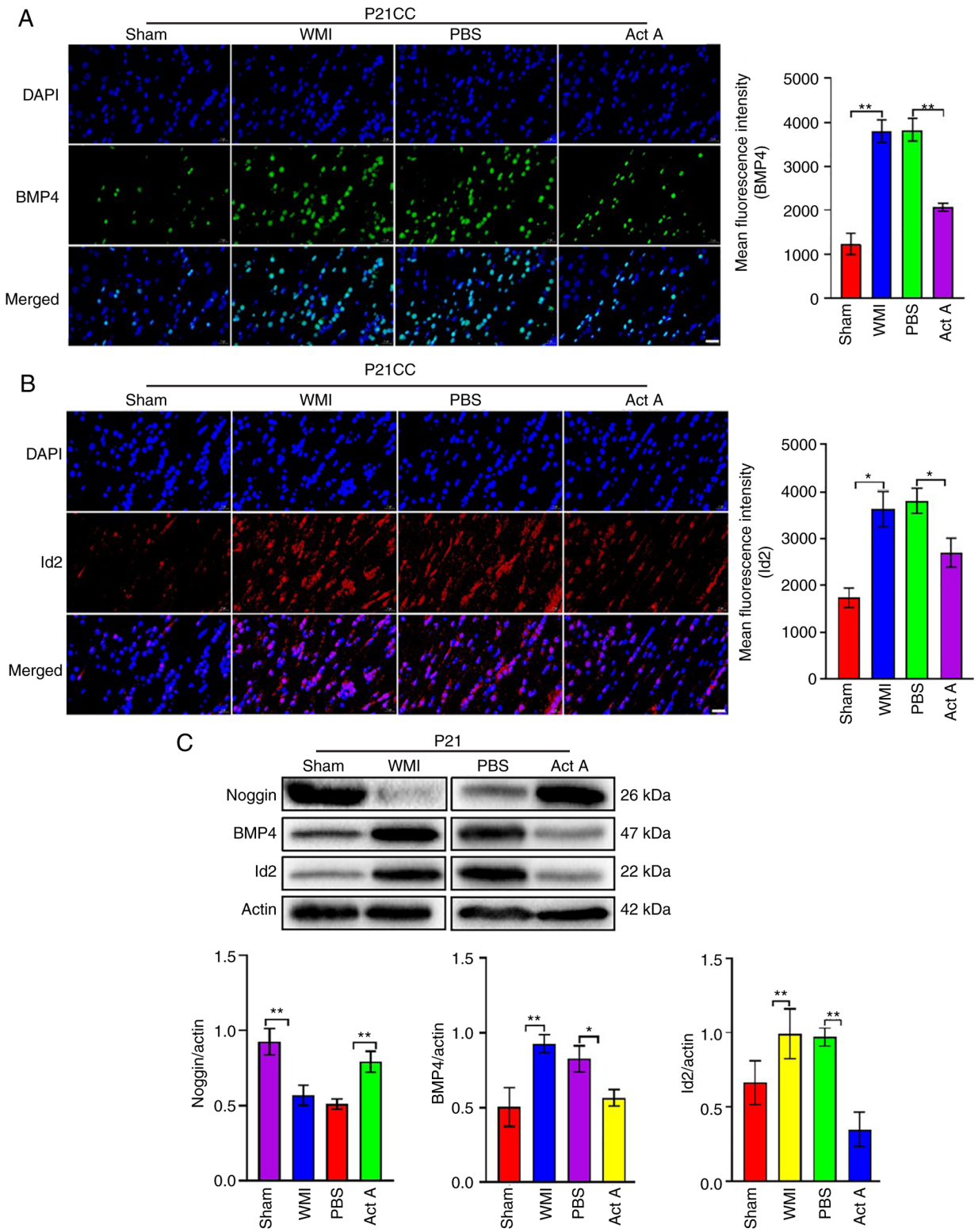

Figure 6. Act A treatment increases Noggin expression, while inhibited the expression of BMP4 and Id2 in WMI rats. (A) Representative immunofluorescence staining of BMP4 (green) expression at P21. Quantitative analysis of the mean fluorescence intensity of BMP4 was performed. It showed that the expression of BMP4 was significantly decreased in the Act A group compared with the PBS group. Scale bar, 20 μm. (B) Representative immunofluorescence staining of Id2 (red) expression at P21. Quantitative analysis of the mean fluorescence intensity of Id2 was performed. It showed that the expression of Id2 was significantly decreased after Act A treatment. Scale bar, 20 μm. (C) Western blot analysis was performed to quantify the expression of Noggin/BMP4/Id2 at P21. It showed that the expression of Noggin was significantly upregulated in the Act A group compared with the PBS group, while BMP4/Id2 was significantly downregulated. *P<0.05 and **P<0.001. Act A, Activin A; WMI, white matter injury; BMP4 expression of bone morphogenetic protein 4; Id2, inhibitor of DNA binding 2.

a useful experimental approach, the invasive nature of this operation limits its clinical applicability. Recently, several non-invasive methods to deliver drugs to the brain and overcome the BBB have emerged, predominantly employing material-based deliveries. For example, Wang *et al* (16) effectively delivered glial cell-derived neurotrophic factor

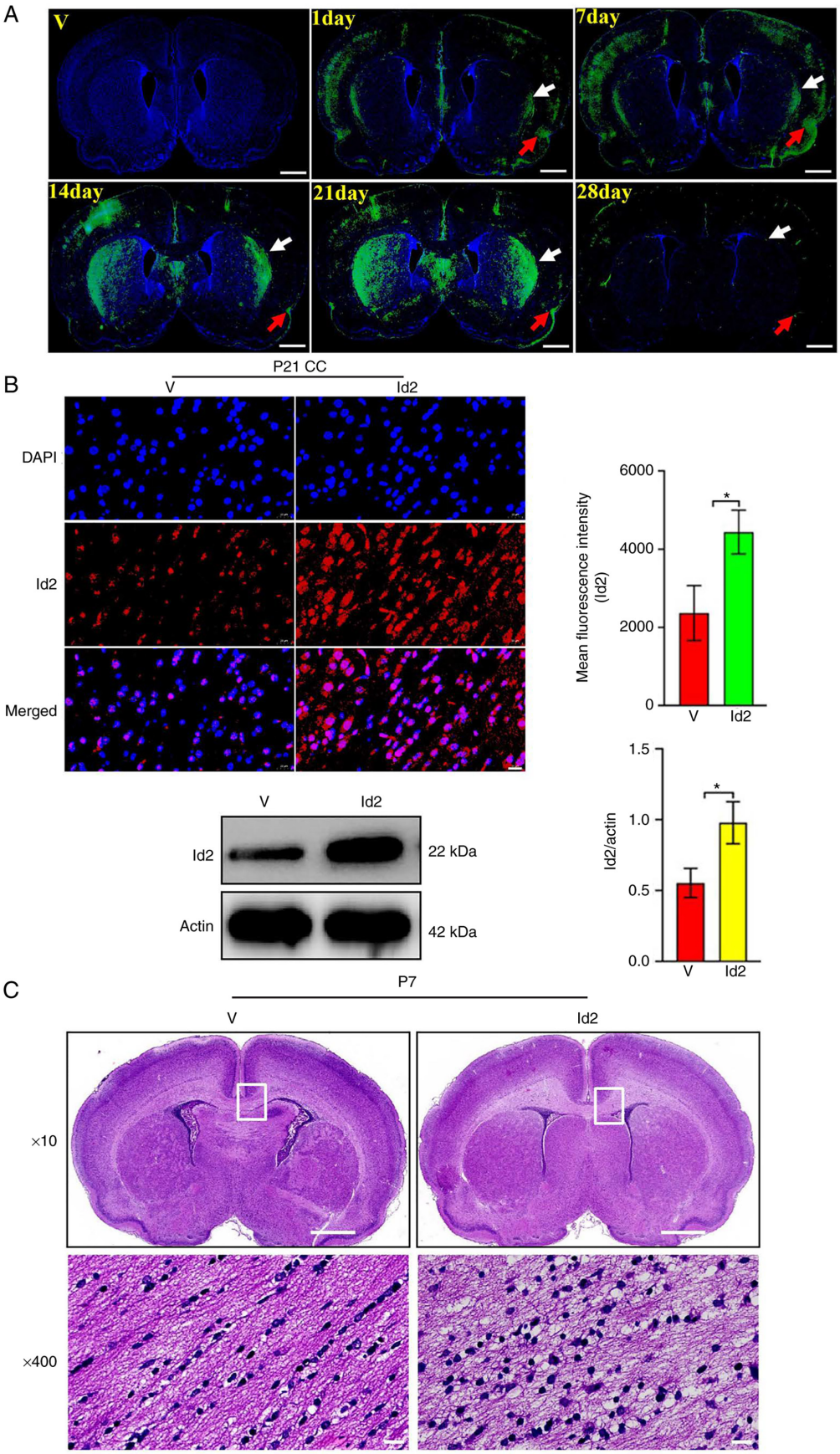

Figure 7. Upregulation of Id2 abolishes the pathological improvement of Act A in white matter injury. (A) Immunofluorescence for Id2-EGFP expression. Arrows indicate the Id2-EGFP (green fluorescence) positive expression. Scale bar, 1,000 μm. (B) Immunofluorescence staining and western blotting to detect the expression of Id2 (red) at P21. It showed that Id2 expression was significantly increased in the Id2 group compared with the V group. V/Id2, group in which vehicle/Id2 overexpression lentiviral vector was injected after 6 h of Act A treatment. Scale bar, 20 μm. (C) H&E staining to evaluate the histopathologic characteristics in the V and Id2 group at P7, which showed more white matter vacuolization and nuclear fragmentation in the Id2 group compared with the V group. Scale bar, 1,000 or 20 μm. *P<0.05. Id2, inhibitor of DNA binding 2; Act A, Activin A.

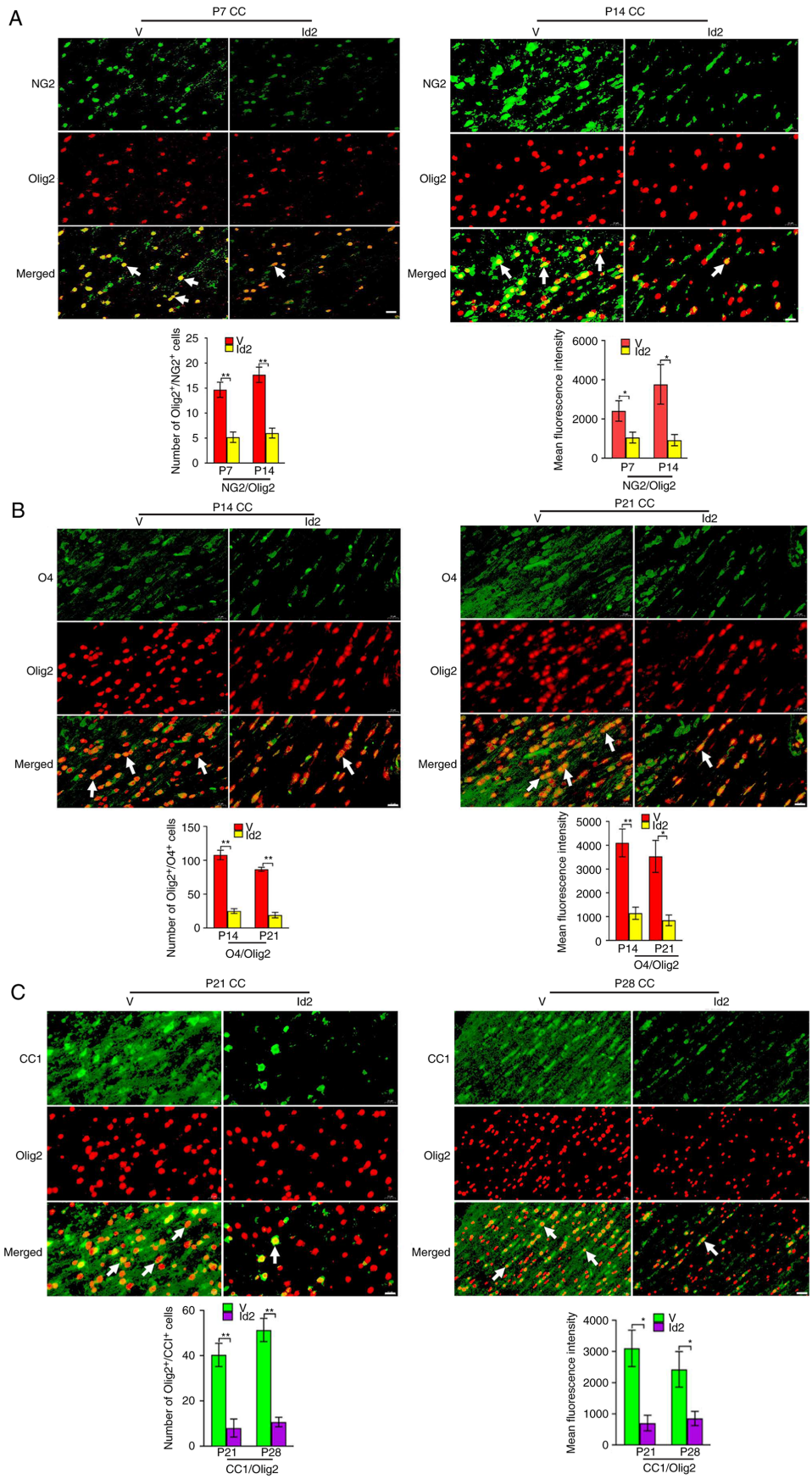

Figure 8. Upregulation of Id2 inhibits oligodendrocyte progenitor cell differentiation. (A) Representative immunofluorescence staining images of NG2 (green) expression via double staining with Olig2 (red) at P7 and P14. Arrows indicate the NG2/Olig2 (yellow) positive cells. Scale bar, 20 μm. (B) Representative immunofluorescence staining images of O4 (green) expression via double staining with Olig2 (red) at P14 and P21. Arrows indicate the O4/Olig2 (yellow) positive cells. Scale bar, 20 μm. (C) Representative immunofluorescence staining images of CC1 (green) expression via double staining with Olig2 (red) at P21 and P28. Arrows indicate the CC1/Olig2 (yellow) positive cells. Scale bar, 20 μm. *P<0.05 and **P<0.001. Id2, inhibitor of DNA binding 2; Olig2, oligodendrocyte transcription factor; NG2, neural/glial antigen 2; CC, corpus callosum.

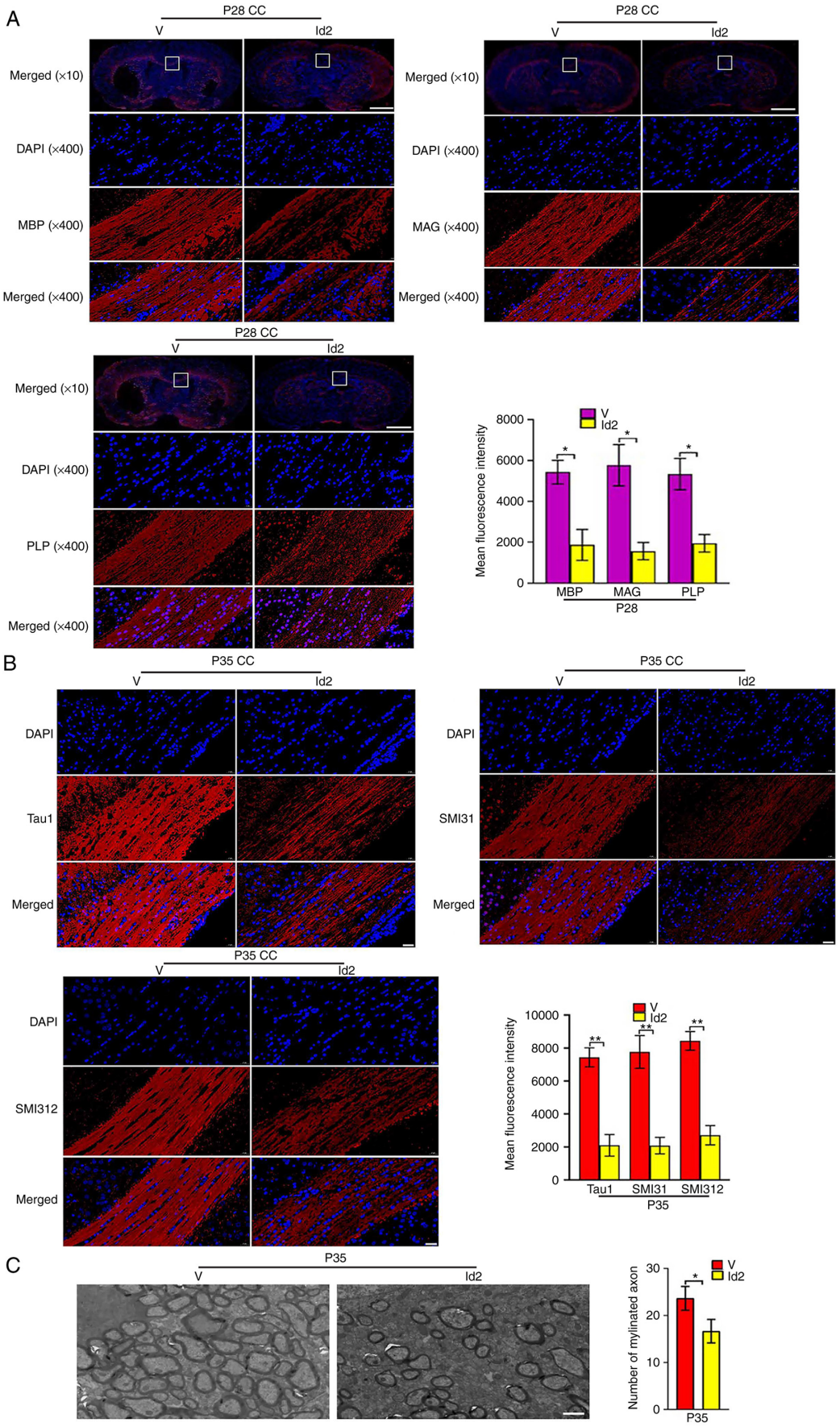

Figure 9. Upregulation of Id2 attenuates the roles of Activin A on myelination and axon formation. (A) Representative immunofluorescence staining images of the expression of myelin sheath markers MBP, PLP and MAG (red) at P28. Scale bar, 1,000 or 20 μm. (B) Representative immunofluorescence staining images of the expression of axon markers Tau1, SMI31 and SMI312 (red) at P35. Scale bar, 20 μm. (C) Representative electron microscopy images at P35. It showed that the Id2 group with less myelinated axons compared with the V group. Scale bar, 2 μm. *P<0.05 and **P<0.001. Id2, inhibitor of DNA binding 2; MBP, myelin basic protein; PLP, proteolipid protein; MAG, myelin-associated glycoprotein.

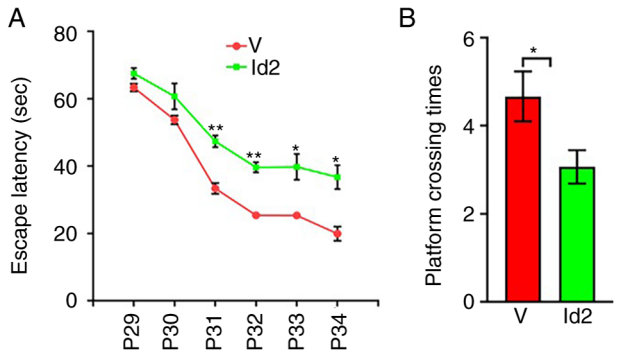

Figure 10. Upregulation of Id2 attenuates the long-time effect of Activin A in white matter injury. (A) Daily average escape latency of SD rats from P29 to P34. It showed that the average escape latency was significantly increased in the Id2 group compared with the V group. (B) The average platform crossing times of SD rats at P35. It showed that the frequency of platform crossing was significantly decreased in the Id2 group compared with the V group. *P<0.05 and **P<0.001. Id2, inhibitor of DNA binding 2.

to the brain of rats via conjugated-biotinylated lipid-coated microbubbles. Other feasible pathways to deliver Act A into the brain shall be investigated in future studies by the authors.

Axons in the vertebrate central nervous system (CNS) are generally ensheathed by myelin, a tight spiral wrapping of plasma membrane generated by OLs (13). Myelin-wrapped axons are the major mediators of signal transduction in the CNS, and their formation is fundamental for brain development and function (13). In accordance with the developmental characteristics of the rat brain, the formation of myelin sheath wrapping axons involves several successive stages, starting from OPC differentiation (17,18). In the present study, different time periods were set to detect the progressive differentiation and maturation of OLs: P7 and P14 to detect OPCs, P14 and P21 to detect pre-OLs, P21 and P28 to detect OLs, P28 to detect myelin formation, and P35 to detect myelin-wrapped axons. This experimental design allowed the authors to obtain an overall view of the effects of Act A on WMI progression. The results of the present study indicated that Act A treatment promoted myelination and axon formation after WMI. It was concluded that this was owing to the alleviation of the OPC differentiation barrier in WMI by Act A treatment, which, in turn, increased the formation of mature OLs to support the formation of myelin and myelinated axons. Further, the MWM test was used to detect behavioral performance reflecting the long-time effects of Act A after WMI. The MWM aims to assess learning and memory ability by analyzing the average escape latency and frequency of platform crossings. The average escape latency was significantly lower whereas the frequency of platform crossings was significantly higher in the Act A group than in the PBS group. These results indicated that Act A treatment improved learning and memory ability in WMI rats, illustrating that Act A treatment enhanced long-time behavioral performance after WMI. The persistent positive effects of Act A after WMI may involve a cascade of events, as follows. First, Act A alleviated the differentiation barrier of OPCs in WMI, which, in turn, increased the formation of mature OLs. After reaching a sufficient number, OLs contributed to myelination and formation of myelinated axons, thereby alleviating pathological damage caused by WMI-induced OPC damage. This ultimately resulted in signal transduction in myelinated axons returning to a normal state reflecting behavioral performance.

A previous study revealed that Act A exerted its neuroprotection roles mainly through the Smad-dependent pathways (19). By contrast, a previous study stated that Act A exerted its effects through Smad-independent pathways, such as nuclear factor-κB, extracellular signal-regulated kinase, ubiquitin-proteolytic, mitogen-activated protein kinase, AKT, and TGF signaling pathways (20). The present study revealed that the reparative effects of exogenous Act A after WMI in newborn rats was predominantly achieved by promoting the differentiation and maturation of OLs. Previous RNA-sequencing experiments on WMI, which indicated that Id2 was a negative regulator of OL maturation, provided clues to explore potential pathways for the roles of Act A in WMI (SU *et al*, unpublished data). Moreover, studies have reported that Id2 participates in different stages of OL differentiation and is a key regulator of OL differentiation and maturation (21,22). Id2 inhibits the expression of myelin formation genes and maintains OPCs in an undifferentiated state, thereby inhibiting OPC differentiation and production of mature OLs (23). Based on this evidence, the KEGG pathway website was searched to elucidate the relationship between Act A and Id2. It was identified that Act A regulated cell differentiation and neurogenesis via the Noggin/BMP/Id signaling pathway. Indeed, several studies have reported that Act A regulates cell differentiation by interacting with BMP4 (24-27), and BMP4, in turn, regulates the differentiation and maturation of OLs by regulating its downstream target molecule Id2. BMP4/Id2 signaling hinders the differentiation of OPCs into OLs (28). Noggin is a key upstream molecule regulated by BMP4. Increased noggin expression inhibits BMP4 expression, whereas Act A enhances noggin expression (29). Based on these data, it was hypothesized that the effects of Act A on WMI may be achieved via Noggin/BMP4/Id2 signaling.

To test the aforementioned hypothesis, the expression of Noggin/BMP4/Id2 after HI or Act A treatment was analyzed and it was observed that noggin expression was inhibited, whereas BMP4 and Id2 expression was increased after HI. After Act A treatment, noggin expression was significantly upregulated, whereas BMP4 and Id2 expression was significantly downregulated. Moreover, Id2 upregulation blocked the rescuing effects of Act A after WMI. Collectively, these results suggested that Act A rescues WMI via the Noggin/BMP4/Id2 signaling pathway. Mechanistically, it was hypothesized that Act A enters the intercellular space through diffusion after injection into the LV and binds to Act A receptors on the surface of OPCs. Subsequently, Act A activates noggin expression and inhibits BMP4 and Id2 expression. This relieves the negative regulatory factors that modulate OPC differentiation, promotes myelin sheath formation, reduces pathological white matter damage in the brain, and rescues neurobehavioral defects in rats. However, the effects of blocking or overexpressing noggin and BMP4 have not been verified. Hence, this remains speculative, and more research is warranted to verify the causal relationship between Act A-mediated regulation of Id2 and Noggin/BMP4 signaling.

In summary, the present study demonstrated that exogenous Act A treatment rescued WMI via the Noggin/BMP4/Id2 signaling pathway. Although Act A has been used as a diagnostic

and prognostic biomarker for several brain diseases (30), it has not been used to treat brain damage in clinical practice. The present findings demonstrated for the first time, to the best of our knowledge, that exogenous Act A treatment may alleviate WMI in the neonatal rat brain, highlighting the potential of using Act A as a therapeutic agent to treat neonatal WMI. Besides, the encephalopathy of prematurity conceived by Volpe (31) indicated that it is a complex amalgam of primary destructive disease and secondary maturational and trophic disturbances. The aforementioned study claimed that the neuropathology of brain injury in the premature infant occurs against a background of multiple active developmental events that take place at 24-40 weeks of gestation and involve pre-OLs, microglia, axons, subplate neurons, the proliferative cerebral dorsal subventricular zone and ventral germinative epithelium of the ganglionic eminence, thalamus, cortex and cerebellum (31). In the present study, the treatment roles and mechanisms of Act A against the background of human fetuses aged 23-32 weeks that within the duration of the preterm infants described in Volpe (31) were explored; the main characteristics of the aforementioned fetuses are the obstacle of OPCs differentiation, which finally leads to the behavioral and cognitive dysfunction. Thus, the pathological characteristics, oligodendrocyte lineage cells, the myelination, axon formation and the behavioral and cognitive ability were established as the primary study index. The present findings indicated that Act A ameliorated the pathological damages, promoted the differentiation of OPCs, improved the myelination and axon formation, and finally rescued the learning and memory abilities, of which hinted that Act A not only influence the primary destructive disease but also the secondary developmental process. Collectively, the current study concluded that Act A shows rescue effects in premature encephalopathy of 23-32 weeks. Regarding the effective roles of Act A in the primary destructive disease and the secondary maturational process, it is hypothesized that Act A may also play roles during the encephalopathy of prematurity of 24-40 weeks. Besides, it is considered that the types of pathological changes, the involved tissues and severity of neuro injury are more complex between the large extents of 24-40 weeks, which needs further validation.

Acknowledgements

Not applicable.

Funding

The present study was supported by the National Key R&D Program of China (grant nos. 2021YFC2701704 and 2017YFA0104200), the National Natural Science Foundation of China (grant nos. 81971433 and 81971428), the Science and Technology Bureau of Sichuan Province (grant nos. 2021YJ0017 and 2020YFS0041), the Fundamental Research Funds for Central University (grant no. SCU2021D009) and the National Key Project of Neonatal Children (grant no. 1311200003303).

Availability of data and materials

All data generated or analyzed during this study are included in this published article.

Authors' contributions

XS and JY contributed to the conception and design of the research and drafting of the present study. DX and XQ performed the MWM test. SL and FZ participated in data acquisition. JT made substantial contributions to the conception, design, acquisition, analysis and interpretation of data and revised the manuscript. XS and JT confirm the authenticity of all the raw data. All authors read and approved the final version of the manuscript.

Ethics approval and consent to participate

All animal experiments were approved (approval no. WCSUH21-2018-034) by the Sichuan University Committee on Animal Research (Chengdu, China) and complied with the ARRIVE guidelines.

Patient consent for publication

Not applicable.

Competing interests

The authors declare that they have no competing interests.

References

1. Alexandrou G, Mårtensson G, Skiöld B, Blennow M, Adén U and Vollmer B: White matter microstructure is influenced by extremely preterm birth and neonatal respiratory factors. Acta Paediatr 103: 48-56, 2014.
2. Liu XB, Shen Y, Plane JM and Deng W: Vulnerability of premyelinating oligodendrocytes to white-matter damage in neonatal brain injury. Neurosci Bull 29: 229-238, 2013.
3. Gano D: White matter injury in premature newborns. Neonatal Netw 35: 73-77, 2016.
4. Suzuki N, Sekimoto K, Hayashi C, Mabuchi Y, Nakamura T and Akazawa C: Differentiation of oligodendrocyte precursor cells from Sox10-venus mice to oligodendrocytes and astrocytes. Sci Rep 7: 14133, 2017.
5. Anand C, Brandmaier AM, Arshad M, Lynn J, Stanley JA and Raz N: White-matter microstructural properties of the corpus callosum: Test-retest and repositioning effects in two parcellation schemes. Brain Struct Funct 224: 3373-3385, 2019.
6. Goebbels S, Wieser GL, Pieper A, Spitzer S, Weege B, Yan K, Edgar JM, Yagensky O, Wichert SP, Agarwal A, *et al*: A neuronal PI(3,4,5)P_3-dependent program of oligodendrocyte precursor recruitment and myelination. Nat Neurosci 20: 10-15, 2017.
7. Wang X, Fischer G and Hyvönen M: Structure and activation of pro-activin A. Nat Commun 7: 12052, 2016.
8. Zheng J, Zhang T, Han S, Liu C, Liu M, Li S and Li J: Activin A improves the neurological outcome after ischemic stroke in mice by promoting oligodendroglial ACVR1B-mediated white matter remyelination. Exp Neurol 337: 113574, 2021.
9. Clancy B, Darlington RB and Finlay BL: Translating developmental time across mammalian species. Neuroscience 105: 7-17, 2001.
10. Huang L, Zhao F, Qu Y, Zhang L, Wang Y and Mu D: Animal models of hypoxic-ischemic encephalopathy: Optimal choices for the best outcomes. Rev Neurosci 28: 31-43, 2017.
11. Huang Z, Liu J, Cheung PY and Chen C: Long-term cognitive impairment and myelination deficiency in a rat model of perinatal hypoxic-ischemic brain injury. Brain Res 1301: 100-109, 2009.
12. Wang F, Yang YJ, Yang N, Chen XJ, Huang NX, Zhang J, Wu Y, Liu Z, Gao X, Li T, *et al*: Enhancing oligodendrocyte myelination rescues synaptic loss and improves functional recovery after chronic hypoxia. Neuron 99: 689-701.e5, 2018.

13. Snaidero N, Möbius W, Czopka T, Hekking LH, Mathisen C, Verkleij D, Goebbels S, Edgar J, Merkler D, Lyons DA, *et al*: Myelin membrane wrapping of CNS axons by PI(3,4,5)P3-dependent polarized growth at the inner tongue. Cell 156: 277-290, 2014.
14. De Berdt P, Bottemanne P, Bianco J, Alhouayek M, Diogenes A, Lloyd A, Llyod A, Gerardo-Nava J, Brook GA, Miron V, *et al*: Stem cells from human apical papilla decrease neuro-inflammation and stimulate oligodendrocyte progenitor differentiation via activin-A secretion. Cell Mol Life Sci 75: 2843-2856, 2018.
15. Nishio S, Yunoki M, Chen ZF, Anzivino MJ and Lee KS: Ischemic tolerance in the rat neocortex following hypothermic preconditioning. J Neurosurg 93: 845-851, 2000.
16. Wang F, Shi Y, Lu L, Liu L, Cai Y, Zheng H, Liu X, Yan F, Zou C, Sun C, *et al*: Targeted delivery of GDNF through the blood-brain barrier by MRI-guided focused ultrasound. PLoS One 7: e52925, 2012.
17. Simons M and Nave KA: Oligodendrocytes: Myelination and axonal support. Cold Spring Harb Perspect Biol 8: a020479, 2015.
18. Back SA: White matter injury in the preterm infant: Pathology and mechanisms. Acta Neuropathol 134: 331-349, 2017.
19. Zhang Y, Zhang J, Navrazhina K, Argaw AT, Zameer A, Gurfein BT, Brosnan CF and John GR: TGFbeta1 induces Jagged1 expression in astrocytes via ALK5 and Smad3 and regulates the balance between oligodendrocyte progenitor proliferation and differentiation. Glia 58: 964-974, 2010.
20. Derynck R and Zhang YE: Smad-dependent and Smad-independent pathways in TGF-beta family signalling. Nature 425: 577-584, 2003.
21. Chen XS, Zhang YH, Cai QY and Yao ZX: ID2: A negative transcription factor regulating oligodendroglia differentiation. J Neurosci Res 90: 925-932, 2012.
22. Gou X, Tang Y, Qu Y, Xiao D, Ying J and Mu D: Could the inhibitor of DNA binding 2 and 4 play a role in white matter injury? Rev Neurosci 30: 625-638, 2019.
23. Samanta J and Kessler JA: Interactions between ID and OLIG proteins mediate the inhibitory effects of BMP4 on oligodendroglial differentiation. Development 131: 4131-4142, 2004.
24. Kim MS, Horst A, Blinka S, Stamm K, Mahnke D, Schuman J, Gundry R, Tomita-Mitchell A and Lough J: Activin-A and Bmp4 levels modulate cell type specification during CHIR-induced cardiomyogenesis. PLoS One 10: e0118670, 2015.
25. Olsen OE, Wader KF, Hella H, Mylin AK, Turesson I, Nesthus I, Waage A, Sundan A and Holien T: Activin A inhibits BMP-signaling by binding ACVR2A and ACVR2B. Cell Commun Signal 13: 27, 2015.
26. Yang S, Yuan Q, Niu M, Hou J, Zhu Z, Sun M, Li Z and He Z: BMP4 promotes mouse iPS cell differentiation to male germ cells via Smad1/5, Gata4, Id1 and Id2. Reproduction 153: 211-220, 2017.
27. Lepletier A, Hun ML, Hammett MV, Wong K, Naeem H, Hedger M, Loveland K and Chidgey AP: Interplay between follistatin, activin A, and BMP4 signaling regulates postnatal thymic epithelial progenitor cell differentiation during aging. Cell Rep 27: 3887-3901.e4, 2019.
28. Miyazono K and Miyazawa K: Id: A target of BMP signaling. Sci STKE 2002: pe40, 2002.
29. Koyano S, Fukui A, Uchida S, Yamada K, Asashima M and Sakuragawa N: Synthesis and release of activin and noggin by cultured human amniotic epithelial cells. Dev Growth Differ 44: 103-112, 2002.
30. Bergestuen DS, Edvardsen T, Aakhus S, Ueland T, Oie E, Vatn M, Aukrust P and Thiis-Evensen E: Activin A in carcinoid heart disease: A possible role in diagnosis and pathogenesis. Neuroendocrinology 92: 168-177, 2010.
31. Volpe JJ: Brain injury in premature infants: A complex amalgam of destructive and developmental disturbances. Lancet Neurol 8: 110-124, 2009.